Environmental Engineering and Management Journal *March 2020, Vol. 19, No. 3, 453-466*
http://www.eemj.icpm.tuiasi.ro/; http://www.eemj.eu

"Gheorghe Asachi" Technical University of Iasi, Romania

ZINC HYDROXIDE NANOPARTICLES-MODIFIED CLAY FOR ULTRASOUND-ASSISTED REMOVAL OF METHYLENE BLUE

Adel Valipour[1], Fatemeh Abbasitabar[2], Vahid Zare-Shahabadi[1*]

[1]*Department of Chemistry, Mahshahr Branch, Islamic Azad University, Mahshahr, Iran*
[2]*Department of Chemistry, Marvdasht Branch, Islamic Azad University, Marvdasht, Iran*

Abstract

The objective of the present work was to introduce a novel adsorbent with high adsorption potential toward methylene blue by decorating montmorillonite clay (MMT clay) with $Zn(OH)_2$–nanoparticles ($Zn(OH)_2$–NPs). The adsorbent was characterized structurally by FE-SEM and FTIR techniques. Central composite design–response surface methodology was applied to optimize experimental variables including adsorbent dosage, pH, initial MB concentration, NaCl concentration, and sonication time. A modified quadratic model was used to establish a relationship between the removal percent of MB and the experimental variables. F–value of 74.99 and squared correlation coefficient of 0.96 confirmed the significance and reliability of the model. Under the optimum conditions of pH 8.0, sonication time 3.5 min, adsorbent dosage 73 mg, analyte concentration 7.5 mg L^{-1}, and electrolyte concentration (2 % w/v), the removal percentage of 99.3± 0.70 % were attained. Freundlich isotherm was agree well with the adsorption isotherm data. The adsorption kinetic was best described by pseudo second–order kinetic model. Thermodynamic study of the MB uptake on the sorbent shows the spontaneous ($\Delta G = -13.45 - -34.15$ kcal mol^{-1} in the temperature range of 15–45 °C). These results infer that Zn(OH)2–NPs–MMT clay can be applied as a new, low cost adsorbent in adsorbing MB from aqueous solution.

Key words: cationic dye, multilayer adsorption isotherm, response surface plots, ultrasound assisted adsorption, zinc hydroxide

Received: June, 2019; Revised final: August, 2019; Accepted: October, 2019; Published in final edited form: March, 2020

1. Introduction

The majority of public and authorities concern about rising the environmental pollution which seriously threatens the health of humans and other living beings. Contaminants due to dye have attracted great attention over the past decades. Dyes are extensively used in tanning, pharmaceuticals, paper, plastics, textiles, and food processing industries and consequently a large amount of them is discharged to the environment (Sun et al., 2014; Vasques et al., 2014; Willett et al., 2019). The presence of dyes pose not only an aesthetically unpleasant environment, but also many of them have adverse effects on human health owing to their high toxicity and potential mutagenic/carcinogenic (Wong et al., 2016; Yu et al., 2015) and aquatic ecosystems by preventing light penetration into the water (Nassar and Magdy, 1997). Dye toxicity depends on its type and the obtained products through its metabolic breakdown (Xu et al., 2007). However, the treatment process of wastewater containing dyes is very difficult, since dye design is such that it resist to light, heat, oxidizing agents, and aerobic digestion (Talarposhti et al., 2001).

In respect to worries about the health risks related to the use of dyes, several physical, chemical and biological methods like adsorption, electro–coagulation, ozone–assisted chemical oxidation, membrane, and so on have been applied to protect aquatic environment by eliminating industrial wastes (Secula et al., 2018; Xu et al., 2016; Xu et al., 2017; Zhang et al., 2017). Adsorption is generally the

* Author to whom all correspondence should be addressed: e-mail: valizare@gmail.com; Phone: +98 9125675301; Fax: +98 7137328581

superior and most proficient method for reducing the concentration of dyes in an effluent way, because of high capacity, ease of operational, simplicity, nontoxic, economic feasibility, efficient adsorption and no sludge formation (Guo et al., 2014; Tsai et al., 2007). Commercially available activated carbon has been recognized as an appropriate and successful sorbent to treat dyes due to its high capacity, chemical nature of its surface, and microporous character. Unfortunately, some drawbacks such as poor ability of regeneration and high production cost restricts its use in industrial scale (Tsang et al., 2007). Because of this limitations, it is still a great challenge to develop cheaper and more efficacious adsorbent and overcome these shortcomings.

In recent years, natural clays as cost–effective and easily available material have been broadly applied on organic dye wastewater, heavy metals, and organic compounds (Bergaya and Lagaly, 2006; Bilgiç, 2005; Murray, 2000; Tahir and Rauf, 2006). Clays have interesting features like low cost, a large surface-area-to-mass ratio, chemical and mechanical stability, high cation exchange capacity, high removal efficiency, high thermal stability, high removal efficiency, non–toxicity, and ecosystem friendly (Liu and Zhang, 2007). Clay materials are sandwiches of octahedral sheet of alumina and tetrahedral sheet of silica. They are categorized into different types according to the number of octahedral and tetrahedral layers. The negative charge on the clays is originated from different sources. A negative surface charge creates on the clays as a result of isomorphous substitution of Si^{4+} in tetrahedral layers by Al^{3+} and Al^{3+} in octahedral layers by Mg^{2+} and is very dependent on the type of the clay. The second source of negative charge is the dissociation of hydrogens in Si–OH and Al–OH groups. Edge atoms with low coordination number also cause negative charge. Cations such as sodium and calcium placed in the interlayer spaces compensate the negative charge and bring about major sorption properties (Miyamoto et al., 2000; Shawabkeh and Tutunji, 2003; Skipper et al., 1995). The anionic layers attract heteroaromatic cationic dyes on their own side and are, therefore, quite suitable to fix pollutants from aqueous solutions (Cione et al., 1998). Nevertheless, the sorption capacity of clays is usually less than those of synthetic sorbents and could be enhanced for applied operation. Thus, various treatment processes have been applied to develop the capacity of the clays such as treatment by organic and inorganic compounds, acids and bases. The treatment conditions and the nature of the clay material have great effects on the mineralogical structure and the chemical composition of clay (Ahenach et al., 1998; Espantaleon et al., 2003; Oliveira et al., 2003; Pradas et al., 1994; Tahir and Rauf, 2006; Unuabonah et al., 2007). Nowadays, nanomaterials have widely studied to improve adsorption properties of the adsorbents. Metallic nanostructures like $Cd(OH)_2$ nanowires, Pt nanoparticles, and etc. can be loaded on the adsorbent surface through functional groups on their surfaces and hence improve the surface area and the number of surface reactive atoms (Ghaedi et al., 2013; Ghaedi et al., 2012).

In order to investigate the conditions at which the maximum benefit is achieved, the optimization process is usually performed. The commonly used procedure is one–variable–at–a–time (Araujo and Brereton, 1996). In this method, one parameter is changed and the effect of it is explored on the experimental response while the other parameters are remained constant at a certain level. This optimization technology has some weaknesses. This method does not provide the optimal conditions and also the combined effects between the variables are not considered. In addition, many experiments are necessary to do the research (Mahmoodi and Sargolzaei, 2014). For solving this problems, the optimization procedure can be performed using statistically experiments such as response surface methodology (RSM) as an alternative powerful statistical tool. RSM provides a lot of information with significant reduction in the number of experiment trials along with the description of the relationship between the effective factors and the response (Antony and Roy, 1999) .

In this study, exploring and preparing $Zn(OH)_2$ nanoparticle–modified montmorillonite (MMT) clay nanocomposite was intended for its potential application as a new adsorbent in dye removal. In this regards, $Zn(OH)_2$ nanoparticles were synthesized and loaded on the MMT clay. Methylene blue (MB), a monovalent organic dye, was chosen as a model dye to investigate the applicability of $Zn(OH)_2$ nanoparticles–modified MMT clay as a potential sorbent for dye removal from aqueous solutions. The interaction between methylene blue and clay minerals has been studied extensively (Almeida et al., 2009; Mishael et al., 1999; Rytwo et al., 1995). According to the literature reports, it is the first effort to employ $Zn(OH)_2$–NPs–modified MMT clay as a nanocomposite sorbent in the field of environmental remediation. The synthesized adsorbent was characterized by FE-SEM and FTIR analysis. Among the benefits of the presented work is the utilization of ultrasound irradiation to enhance the rate of adsorption. The ultrasound assisted formation of cavities which can produces intense shockwave when exposed to high compression (Chen et al., 2009; Teng et al., 2014). To improve the performance of $Zn(OH)_2$–nanoparticles–modified MMT clay in MB removal from aqueous solutions, the effect of different operational parameters such as the amounts of sorbent, pH of the solution, initial MB concentration, and sonication time on the removal recovery was modeled and optimized using RSM based central composite design (CCD). The adsorption isotherm data were obtained at three different temperatures and then the best isotherm model was determined by fitting different isotherm equations to the experimental data. Adsorption kinetics were applied with the aim of determining adsorption mechanism. The thermodynamics parameters were calculated by investigating the effects of temperature on the adsorption. The results showed that this new type of nanosorbent has low cost, ease of operation, fast removal and will be useful for wastewater remediation studies.

2. Experimental

2.1. Materials and solutions

Methylene blue ($C_{16}H_{18}N_3SCl$), ammonia, zinc acetate ($Zn(CH_3COO)_2.2H_2O$) (>99.5%), acetic acid, boric acid, and phosphoric acid were all purchased from the Merck Company (Darmstadt, Germany). MMT clay was obtained from Speed Powder Kashan Company (Kashan, Iran). It was ground and sieved over a 120–mesh screen before used. 50 mL of acetate buffer (0.05 mol L^{-1}, pH 5.0) was prepared using sodium acetate and acetic acid. To prepare a universal buffer of 0.1 mol L^{-1}(pH 5.0), 3.42 mL phosphoric acid, 2.86 mL acetic acid, and 3.1 g acid boric were mixed and diluted with double distilled water to 500 mL. Stock methylene blue solution with concentration of 500 mg L^{-1} was prepared by dissolving 250 mg of dye in 500 mL double distilled water. Working solutions were made by diluting the corresponding stock solution. Adjustment pH was carried out with either with 0.1 mol L^{-1} hydrochloric acid or 0.1 mol L^{-1} sodium hydroxide whenever required. All chemicals used were of analytical grades and used as received without further purification. Doubly distilled water was utilized in preparation of all solutions.

2.2. Instrumentation

The pH of the solution was controlled with a Metrohm pH meter (model 691) with a combined double junction glass electrode, calibrated against two standard buffer solutions at pH 4.0 and 7.0. Determination of methylene blue (λ_{max} = 665 nm) in the samples was done using a UV–Vis spectrophotometer (model T80–UV/Vis, PG Instruments Ltd., England). A forced–air drying oven (model 630; National Appliance Co., Portland, Ore.) was employed to dry the samples. Field emission–scanning electron microscope (FE–SEM) was performed by Hitachi S4160 under an acceleration voltage of 15 kV and FTIR spectrum was recorded by Unicam model RS/1. A 37–kHz ultrasonic water bath (Elmasonic E 30 H, 240 W, Elma, Singen, Germany) was used for assisting the adsorption process. Sonication was done at ambient temperature. During sonication, the rise in temperature of the ultrasonic bath was controlled by addition of ice–water (2 °C) to the bath. The experimental design and statistical analysis of the data was performed by using STATISTICA 64 software.

2.3. Preparation of $Zn(OH)_2$–clay

The MMT clay was modified by $Zn(OH)_2$ nanoparticles by the following procedure. Firstly, 0.5328 g of $Zn(CH_3COO)_2.2H_2O$ was dissolved in 100 mL of water. Then 5 mL ammonia solution was added dropwise, and stirred for around 20 min. A white precipitate was formed during this time which would be dissolved by excess addition of ammonia, causing formation of a transparent solution of $Zn(NH_3)_4^{2+}$. The as–prepared solution was transported into an ultrasound bath and 5.0 g clay was added and agitated for 30 minutes. After that, pH of the solution was adjusted at ca.12 by NaOH (0.2 M). Finally, the mixture was kept at room temperature for 10 h, leading to the growth of the $Zn(OH)_2$–NPs on the surface of clay particles. The mixture was filtered, the modified clay was washed with double distilled water, and then dried under air.

2.4. Adsorption procedure

To study the effect of experimental parameters like pH of the sample solution, sonication time, initial dye concentration and electrolyte concentration on the removal of MB, as well as kinetic and thermodynamic characteristics of the adsorbent, some adsorption experiments were conducted. All adsorption experiments were carried out in a batch mode whilst the sample solution was sonicated at optimum conditions suggested by RSM. For a typical experimental run, 50 mL of MB solution at a specified concentration and the optimum pH was completely mixed with a specified amount of adsorbent over a fixed time. During this period, the mixture was agitated by ultrasound and then filtrated. The supernatant was spectrophotometrically quantified for the determination of MB concentration at wavelength of 665 nm. Removal percentage of MB was calculated from a calibration graph. The removal percentage of MB and the corresponding adsorption capacity were calculated using Eqs. (1-2), respectively.

$$\mathrm{R}(\%) = \frac{C_0 - C_e}{C_0} \times 100 \tag{1}$$

$$q_e = \frac{V(C_0 - C_e)}{m} \tag{2}$$

where R is the removal percentage; C_0 and C_e (mg L^{-1}) are the initial and equilibrium MB concentration, respectively; *m* (mg) is the mass of adsorbent; *V* (mL) is volume of MB solution; and q_e (mg/g) indicates the equilibrium adsorption capacity.

2.5. Central composite design and statistical analysis

Central composite design (CCD) was employed to optimize the adsorption process of MB on the $Zn(OH)_2$ nanoparticle–loaded clay. Five variables, namely pH (X_1), sonication time (X_2), adsorbent dosage (X_3), initial concentration of MB (X_4), and NaCl concentration (X_5) at five coded levels were screened by thirty two experimental runs (Table 1).

Variables Coding was carried out, to ease the statistical computations, according to the (Eq. 3) (Hassani et al., 2014).

$$x_i = \frac{X_i - X_0}{\Delta X} \tag{3}$$

where x_i and X_i are coded and real values of the experimental variable, respectively, X_0 is the real value at center point and ΔX shows the difference between maximum and minimum of real values for the experimental variable.

Removal percent as dependent variable was correlated to the five considered factors as independent variables using the second–order quadratic polynomial equation as shown by (Eq. 4).

$$Y = \beta_0 + \sum_{i}^{k} \beta_i x_i + \sum_{j=1}^{k} \beta_j x_j + \sum_{i=1}^{k} \beta_{ii} x_i^2 + \sum_{i=1}^{k} \sum_{i \neq j=1}^{k} \beta_{ij} x_i x_j + \varepsilon \tag{4}$$

where *Y* is the response (dependent variable), β_0, β_i, β_{ii}, β_{ij} are intercept and regression coefficients for the linear, quadratic, and interaction terms, respectively and x is the coded level of experimental factor (Hosseini et al., 2009).

Analysis of variance (ANOVA) was used to assess the quality of the model equation using the statistical parameters like *F* value, squared correlation coefficient (R^2), adjusted determination of coefficient ($R^2_{adjusted}$), and cross validation test (Ghaedi et al., 2016). 3D response surface plots were also employed to investigate the interactions between variables.

Table 1. Experimental parameters and their experimental ranges and levels along with the observed response for MB uptake

Factors	***Range and levels***						
	-α		***-1***		***0***	***1***	***+α***
(X_1) pH	2		4		6	8	10
(X_2) Sonication time (min)	0.5		1.5		2.5	3.5	4.5
(X_3) Adsorbent dosage (mg)	20		40		60	80	100
(X_4) Initial concentration of MB (mg L^{-1})	3		6		9	12	15
(X_5) NaCl concentration (%w/v)	0		2		4	6	8
Runs	X_1	X_2	X_3	X_4	X_5	Removal efficiency (%))	
						Actual	Predicted
1	0	0	0	0	-2	99.24	101.71
2	1	1	1	-1	-1	98.57	97.63
3	0	0	-2	0	0	97.02	96.18
4	1	-1	-1	1	1	94.71	94.9
5	1	-1	-1	-1	-1	95.32	93.96
6	0	0	0	-2	0	76.33	77.68
7	0	0	0	0	0	97.79	97.88
8	-1	-1	1	-1	-1	84.78	83.24
9	-1	1	-1	-1	-1	93.26	94.34
10	1	-1	1	-1	1	95.91	93.8
11	0	2	0	0	0	99.34	97.88
12	1	-1	1	1	-1	88.85	87.63
13	2	0	0	0	0	96.91	97.88
14	-2	0	0	0	0	96.54	97.88
15	-1	-1	-1	-1	1	90.25	90.51
16	-1	1	1	-1	1	78.86	79.4
17	-1	-1	1	1	1	98.27	98.19
18	0	0	0	0	0	97.83	97.88
19	0	0	0	0	2	93.28	94.04
20	1	1	-1	1	-1	99.32	98.74
21	0	0	0	0	0	98.85	97.88
22	1	1	-1	-1	1	88.52	90.12
23	0	0	2	0	0	88.13	88.75
24	0	0	0	0	0	99.45	97.88
25	0	0	0	0	0	99.53	97.88
26	-1	1	-1	1	1	94.47	94.52
27	-1	1	1	1	-1	99.41	102.03
28	0	-2	0	0	0	96.36	97.88
29	0	0	0	2	0	88.05	86.48
30	0	0	0	0	0	99.83	97.88
31	-1	-1	-1	1	-1	97.69	98.36
32	1	1	1	1	1	82.08	83.80

The optimum operating conditions were obtained in the STATISTICA 64 software using desirability function (Malenović et al., 2011).

3. Results and discussion

3.1. Characterization of the $Zn(OH)_2$ nanoparticles–modified clay

The FE–SEM images of the montmorillonite clay surface and the $Zn(OH)_2$ nanoparticles loaded on montmorillonite clay are shown in Fig. 1a–b. As can be seen the surface morphology of the MMT clay is homogeneous and relatively smooth. Fig. 2b shows the detailed morphologies of the $Zn(OH)_2$–NPs loaded on the MMT clay which is relatively homogenous in size distribution.

The size of each $Zn(OH)_2$–nanoparticles is estimated in the range of 20–60 nm. FTIR spectra of MMT clay and the modified MMT clay with $Zn(OH)_2$–NPs is given in Fig. 2a–b. The bands at 3500 and 1611 cm^{-1} are due to –OH stretching of water (Chen et al., 2011; Sharma et al., 2016). Stretching of Al–OH appeared at 3695.5 cm^{-1}. The bands at 1083 and 791 cm^{-1} are due to the stretching mode of Si–O bands. A peak appearing around 508 cm^{-1} in Fig. 2b corresponds to the stretching mode of Zn–O bonds in the spectra of $Zn(OH)_2$–NPs loaded on the MMT clay (Ardekani et al., 2017).

The X-ray diffraction (XRD) pattern of the $Zn(OH)_2$–NPs–MMT clay (Fig. 3a) is composed of distinguish characteristic peaks at 2θ = 20.34, 27.06, 32.90, 36.59, 39.83, 40.84, 41.96, 52.38, 60.50, and 69.22 that can be indexed to (110), (111), (211), (002), (021), (121), (400), (122), (113), and (123) of the Orthorhombic structure of $Zn(OH)_2$–NPs–MMT clay, (JCPDS, No. 00-001-0360), respectively. Fig. S3 shows the XRD patterns for raw and modified clays. Fig. S3 confirms decorating of the MMT clay with $Zn(OH)_2$–NPs. No characteristic peaks of phases such as ZnO–nano particles were detected.

$Zn(OH)_2$–NPs have acidic properties and, as a result, the MMT clay decorated with $Zn(OH)_2$–NPs has different behaviors at different pHs. Explanation of the behavior of the adsorbent can be done using pH at the point of zero charge (pH_{PZC}). To measure pH_{PZC} of the $Zn(OH)_2$–NPs–MMT clay batch equilibration technique was applied (Smičiklas et al., 2000). 100 mg of $Zn(OH)_2$–NPs–MMT clay was quantitatively transferred into 10 mL of 0.10 mol L^{-1} KNO_3 and its pH was adjusted from 2–10 by addition of 0.1 mol L^{-1} HCl or NaOH. Suspension was allowed to equilibrate for 24 h in a shaker thermostated at 25 °C. After filtration final pH was measured again. The value of pH_{PZC} can be determined in the plot of ΔpH (pH_{Final} – $pH_{Initial}$) versus $pH_{Initial}$ at which ΔpH is zero. The value of pH_{PZC} for $Zn(OH)_2$–NPs–MMT clay was measured as pH 4.20 (Fig. 3b).

3.2. Mathematical model and data analysis

In this work, by employing the central composite statistical experiment design and RSM, the influence of five independent variables of pH, sonication time, adsorbent dosage, initial concentration of MB, NaCl concentration, and their interactive impacts on the MB percentage uptake as the dependent variable was explored. Experimental data and the observed responses are presented in Table 1. (Eq. 5) shows the obtained full quadratic model.

$$\begin{aligned} y &= 98.73 + 0.29X_1 - 0.22X_2 - 1.86X_3 + \\ &+ 2.20X_4 - 1.92X_5 - 0.39X_1^2 - 0.11X_2^2 - 1.42X_3^2 - 4.02X_4^2 - 0.50X_5^2 - \\ &- 0.08X_1X_2 + 0.12X_1X_3 - 3.50X_1X_4 - 0.47X_1X_5 - 0.41X_2X_3 + \\ &+ 0.18X_2X_4 - 3.70X_2X_5 - 0.52X_3X_4 + 0.07X_3X_5 + 0.17X_4X_5 \end{aligned} \tag{5}$$

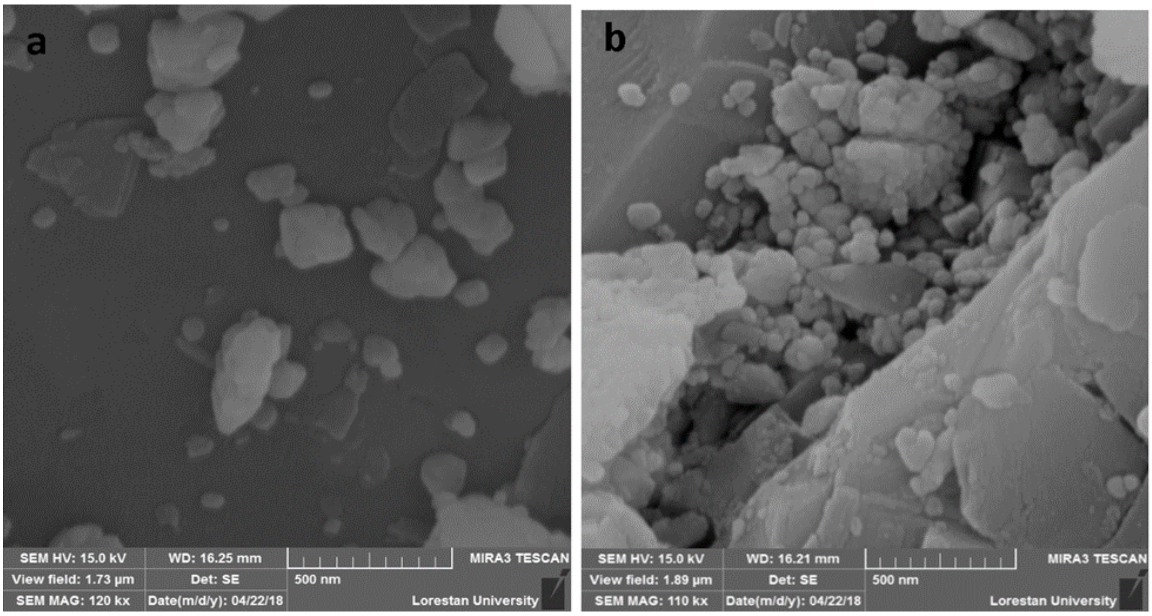

Fig 1. SEM micrograph of a natural clay and b $Zn(OH)_2$–NPs–MMT clay

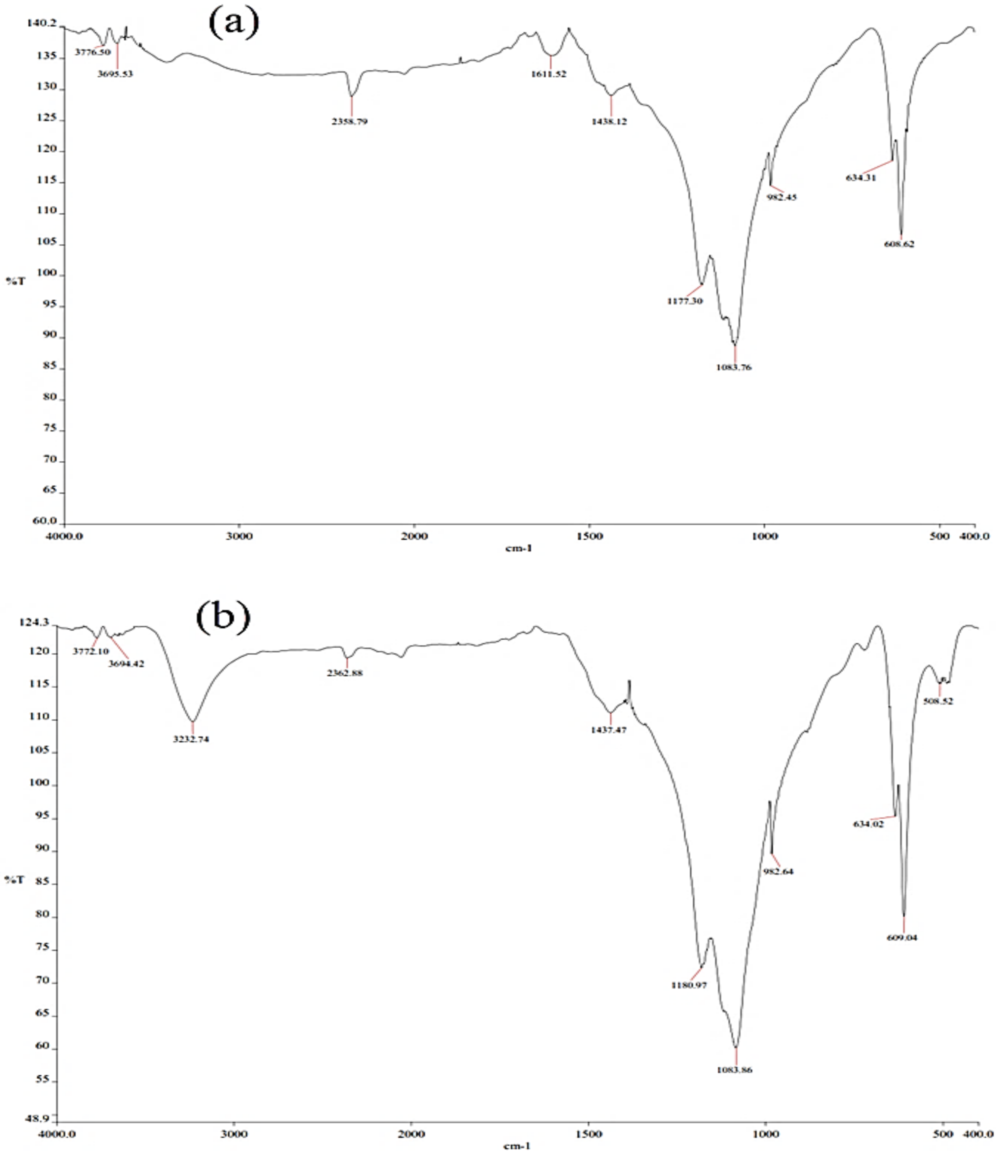

Fig. 2. FTIR spectra of (a) natural clay and (b) Zn(OH)2–NPs–MMT clay

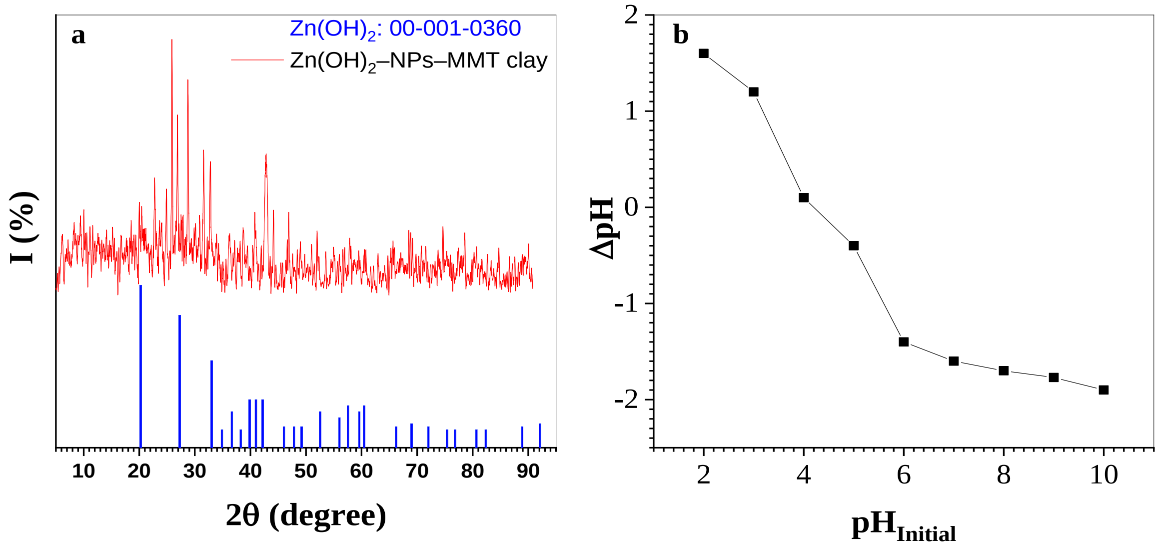

Fig. 3. a. XRD pattern of the $Zn(OH)_2$–NPs–MMT clay; b. pH_{PZC} values of $Zn(OH)_2$–NPs–MMT clay. Condition: $Zn(OH)_2$–NPs–MMT clay 0.1 g; sample volume 50 mL; supporting electrolyte KNO_3 0.1 mol L^{-1}; stirred time: 24 h

The relative significant and interaction of all the variables appeared in the model were evaluated by analysis of variance (ANOVA). The ANOVA table and the corresponding Pareto chart are given in Supplementary information (Table 1 and Fig. 1). Analysis of variance of the full quadratic RSM model showed that there were several non–significant terms (p > 0.05) that should to be removed to obtain a statistically sound model. After removing non–significant terms (Eq. 6) was resulted.

$$Y = 97.88 - 3.72X_3 + 4.40X_4 - 3.84X_5 - \\ -5.41X_3^2 - 15.80X_4^2 - 14.01X_1X_4 - 14.78X_2X_5 \qquad (6)$$

The relative significant and interaction of all the variables appeared in the model were also evaluated by ANOVA (Table 2). Now *p*–value for all terms are less than 0.05, denoting significance of terms at 95% confidence level. *F*–value of the model was 74.99 (compared to the critical value of 2.42 at the 0.05 level of significance) with a *p*–value of 9.2×10^{-15}. In addition, high coefficient of correlation ($R^2 = 0.96$) shows good correlation between the removal efficiency and the independent variables.

Lack of fit (LOF) of 3.41 also implies that model validity is good. The standardized Pareto chart (p=0.05) of the results is shown in Fig. 3a. This Figure depicts the most effective factors on the removal of MB are in the following order of importance: analyte concentration, interaction between time and electrolyte, interaction between pH and analyte, electrolyte, and adsorbent. The normal probability plot of residuals was depicted in Fig. 3b, indicating that all points fell close enough to the straight line. Fig. 3c shows the predicted removal efficiency versus the experimental dat. The response surface plots were provided for a given pair of variables by varying these variables within the experimental ranges while the other variables remain at a constant level. Fig. 4a presents the effect of pH and initial analyte concentration on the removal of MB. It is apparent that at low analyte concentrations, removal percentage of MB linearly increases by pH. At low pHs, surface of the adsorbent gets positive charge due to the protonation. This leads to strong electrostatic repulsion between the positive charges created at surface of the adsorbent and the cationic dye, resulting in diminishing removal percentage of MB. An opposite trend for pH was seen at high analyte concentrations.

Removal percentage of MB in high concentrated solutions decreases linearly with pH. This can be attributed to the aggregation of MB which is exacerbated at high concentrations and high pH values (Yazdani et al., 2012). Moreover, electrostatic interaction between MB dye and $Zn(OH)_2$–NPs–MMT clay is favored at pH > 4.20 because the surface of adsorbent is negatively charged at pHs higher than pH_{PZC} and MB dye are positively charged. Fig. 4b presents effect of electrolyte and sonication time on the removal of MB.

It was found from this figure that at short sonication times, removal efficiency enhanced by addition of an inert electrolyte due to salting out phenomena (Porath et al., 1973). However, removal deceased with electrolyte concentration at higher sonication times which can be explained based on the dimerization reaction of MB. In fact, addition of the electrolyte causes salting out phenomena that helping the removal of MB and intensifies dimerization of MB, as well. At higher sonication times in which the involving components reach the equilibrium, addition of electrolyte causes to decrease of removal due to the dimerization reaction.

3.3. Optimization of CCD by desirability function

The effective factors on MB removal were optimized using the desirability function (DF). Desirability of 1.0 was assigned to the maximum removal (99.83) and 0.0 for the minimum removal (76.33). Desirability of 1.0 was also selected as the target value.

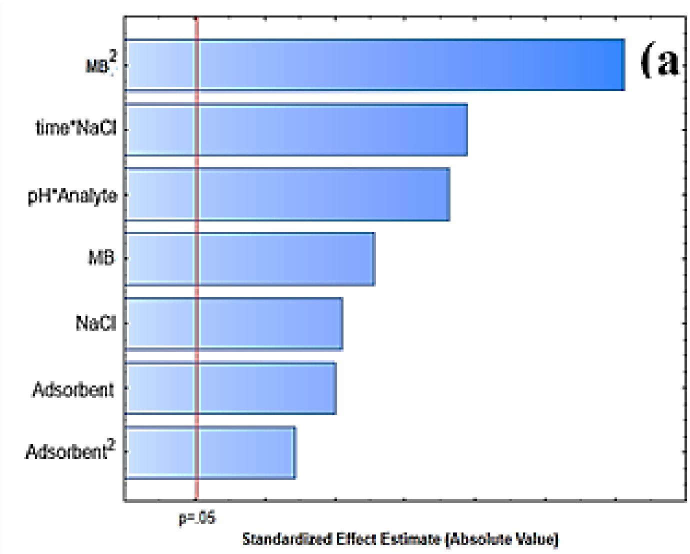

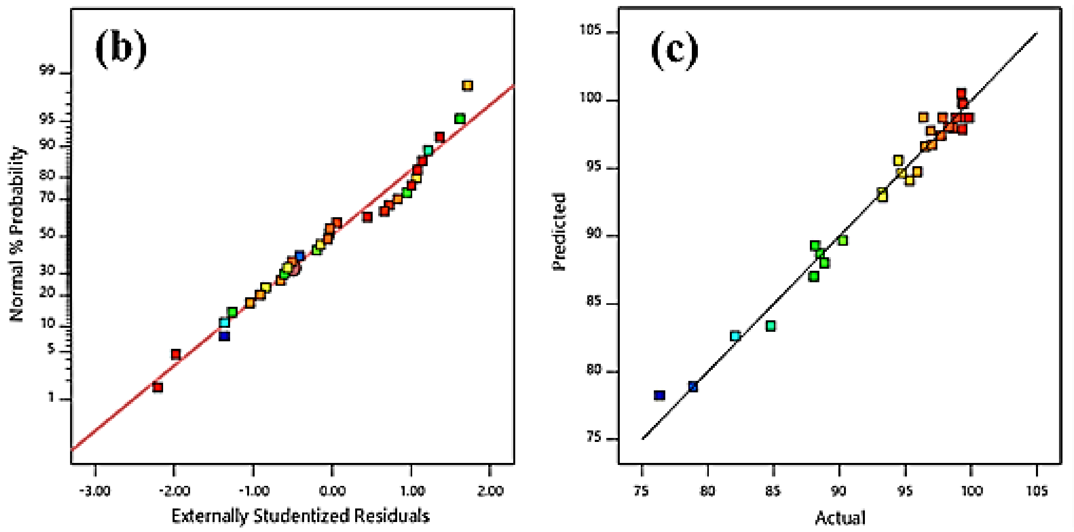

Fig. 3. (a) Standardized Pareto chart. The reference line is shown on the graph. Effect any term that extends past the reference line is significant. ($p < 0.05$); (b) Normal probability plot of residuals; (c) Plotting predicted values of removal versus actual values

Table 2. ANOVA of the modified RSM

Source	*DF*[a]	*Adj SS*	*Adj MS*	*F-value*	*p-value*
Model	7	1203.56	171.94	74.99	0.000
X_3	1	82.84	82.84	36.13	0.000
X_4	1	116.03	116.03	50.60	0.000
X_5	1	88.36	88.36	38.54	0.000
$X3^2$	1	54.68	54.68	23.85	0.000
X_4^2	1	465.83	465.83	203.16	0.000
X_1X_4	1	196.35	196.35	85.64	0.000
X_2X_5	1	218.52	218.52	95.31	0.000
Lack of fit	19	51.09	2.69	3.41	0.089
Pure error	5	3.94	0.79		
Total SS	31	1258.58			
Model Summary Statistics					
S	**R^2**	**Adj-R^2**	**CV %**	**Adeq. Precision**	
1.51	0.9563	0.9435	1.61	32.16	

[a] *DF: degrees of freedom*

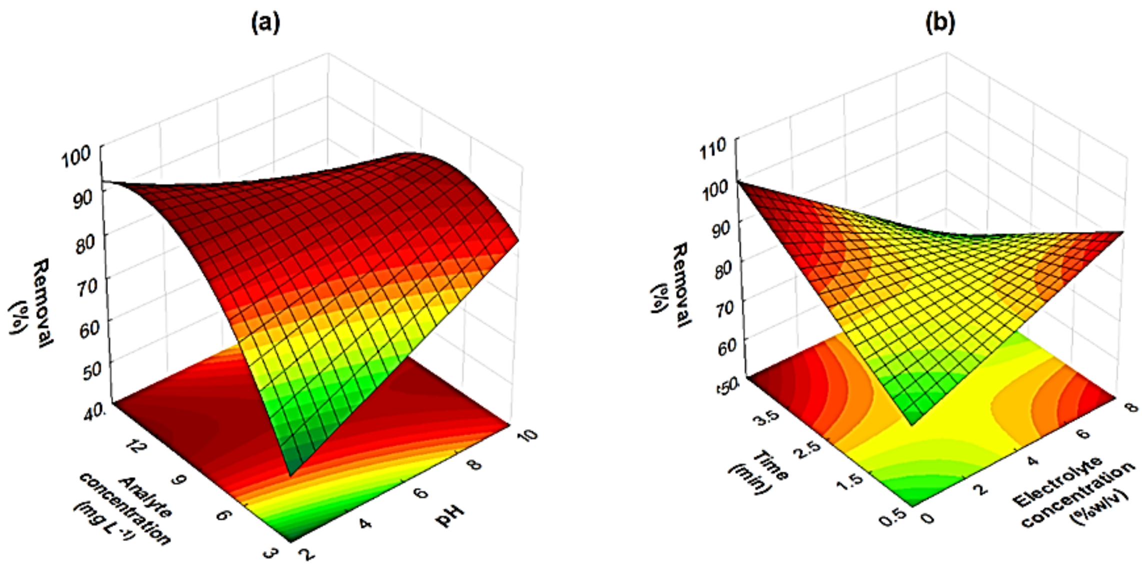

Fig. 4. Response surface plots for the methylene blue removal: (a) Analyte concentration–pH; (b) Time-electrolyte concentration

DF settings for each dependent variable is presented on the right hand side of Fig. 5. At the optimum conditions of pH 8.0, sonication time 3.5 min, adsorbent dosage 73 mg, analyte concentration 7.5 mg L^{-1}, and electrolyte concentration 2 % w/v, maximum removal percentage of MB was achieved.

The optimum conditions were checked by running five replicate experiments under optimum conditions and the removal percentage of 99.3± 0.70 % was obtained.

3.4. Adsorption isotherms

To study the mechanism of adsorption of MB, the experimental data were fitted to Langmuir, Freundlich, Temkin, and multilayer adsorption isotherms. All The resulted parameters and corresponding correlation coefficients for each model are given in Table 3. Fig. S2(a–d) shows plots for all studied isotherms for the adsorption of MB onto the modified clay and the best straight lines representing the fitted points. As can be seen, Temkin model is poorly fitted to the data. Langmuir model was fitted to the data with squared correlation coefficient of 0.84 after removing of some outlier points. The highest fitting was observed for the Freundlich adsorption isotherm with R^2 = 0.99, suggesting that methylene blue adsorption is occurred in multilayer coverage. This fitting signs also that the adsorption of MB on $Zn(OH)_2$–NPs–MMT clay was not by monolayer arrangement.

3.5. Adsorption kinetic studies

Sorption kinetic studies have become imperative due to providing valuable information about mechanism of sorption process and the rate at which the pollutant is removed from the aqueous solution. In addition, it is useful in assessing adsorbent performance. In this work, first and second–order kinetic models were fitted to the obtained experimental kinetic data. The calculated constants of each model along with R^2 values at different initial MB concentrations are given in Table 4.

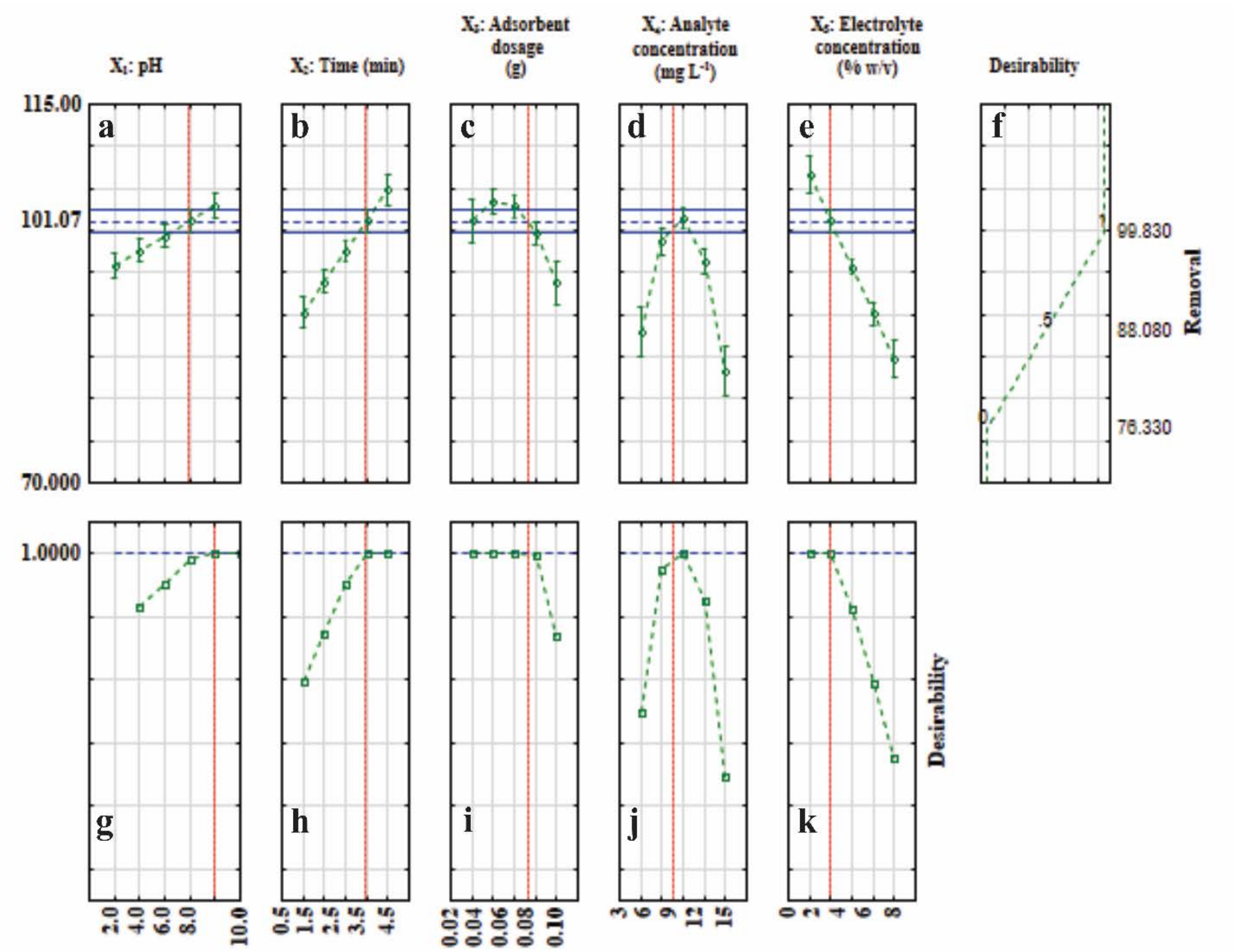

Fig. 5. Profiles for predicated values and desirability function for removal (%) of MB. Dashed line shows current values after optimization: Upper parts of figure show the change in the removal versus (a) pH; (b) time; (c) adsorbent; (d) analyte, (e) electrolyte. Definition of desirability is illustrated in f. The lower parts g–k are desirability changes corresponding to the a–e graphs, respectively

Table 3. Langmuir, Freundlich, Temkin, and multilayer isotherm model constants for the adsorption of methylene blue on the modified clay

Langmuir isotherm model				
K_L	q_m	R_L range	R^2	Equation
1551.6	40.73	0.001-0.162	0.8366	$\frac{1}{q_e}=\frac{1}{q_m}+(\frac{1}{q_m K_L})\frac{1}{C_e}$
Freundlich isotherm model				
K_F	n		R^2	Equation
90.2	3.3		0.9989	$\ln q_e=\ln K_F+\frac{1}{n}\ln C_e$
Temkin isotherm model				
a_t	b_t		R^2	Equation
186.29	19.73		0.7713	$q_e=a_t+b_t\ln C_e$
Multilayer isotherm model				
K_1	K_2	q_m	R^2	Equation
0.39	2.45×10^{-3}	259.9	0.9860	$q_e=\frac{q_m K_1 C_e}{(1-K_2 C_e)\left[1+(K_1-K_2)C_e\right]}$

Based on the calculated R^2 values, it is clear that the pseudo second–order kinetic model is more applicable for description of the adsorption of methylene blue on the modified clay whereas the MB adsorption mechanism on the raw clay is obeyed from the pseudo– first–order model. This observation is consistent with the similar findings on sorption of MB reported (Auta and Hameed, 2014).

3.6. Adsorption thermodynamics

Thermodynamic parameters for adsorption of MB on the modified clay were determined using Eqs. (7-9).

$$\Delta G^{\circ}=-RT\ln K_d \quad (7)$$

$$\ln K_d=\frac{\Delta S^{\circ}}{R}-\frac{\Delta H^{\circ}}{RT} \quad (8)$$

$$K_d=\frac{q_e}{C_e} \quad (9)$$

where: ΔG° is the variation of free energy (kJ mol^{-1}), R is the universal gas constant (8.314 J mol^{-1} K^{-1}), T is the absolute temperature (K), and K_d is the distributed coefficient of solute between the solid and the liquid phase.

The calculated thermodynamic parameters based on the above functions are given in Table 5. From the ΔG° values it was suggested that the adsorption process is spontaneous and feasible in nature. Moreover, the amount of ΔG decreases in going to high temperatures, which shows favorable sorption of MB on the modified clay at high temperatures. The observed ΔH° values were negative, confirming the exothermic nature of the adsorption process. These results indicate that adsorption process of MB onto the prepared $Zn(OH)_2$–modified clay is thermodynamically favorable and are very much comparable to the previously reported works.

3.7. Reusability

Ability to reuse of an adsorbent makes it more economical. With this regard, reusability of the modified clay for the MB adsorption was studied by carrying adsorption and desorption experiments. After adsorption of MB by $Zn(OH)_2$–NPs–MMT clay, the adsorbent was filtered and dried at room temperature. To desorb MB the adsorbent was transferred into 5 mL of 0.01 mol L^{-1} HCl and then sonicated for 3 min. Adsorption experiment was carried out under optimal conditions subsequently; it was observed that $Zn(OH)_2$–NPs–MMT clay gave more than 80% removal of MB dye up to 2 cycles and then efficiency declined to 70% and 55% after third and fourth cycles.

3.8. Comparison with previous studies

The potential of the presented $Zn(OH)_2$–NPs–MMT clay for the removal of MB removal was compared with the previous ones based on maximum adsorption capacity and adsorption time. The adsorption time refers to time allowed to reach the equilibrium. As is seen in Table 6, the adsorption time for the proposed method is superior to the all other adsorbents. The adsorption capacity was also higher than that of 259.9. So, the presented $Zn(OH)_2$–nanoparticles–montmorillonite clay could be considered as an alternative to achieve higher rates and efficiencies for removing of MB.

4. Conclusions

This paper describes an ultrasonic–assisted removal of MB based on a simple, inexpensive adsorption technique using a prepared $Zn(OH)_2$–NPs–MMT clay as adsorbent. Central composite design response surface methodology was employed for experimental design to investigate the effect of five independent variables such as pH, sonication time, adsorbent dosage, initial concentration of MB, and electrolyte concentration.

Table 4. Pseudo-first and pseudo-second order kinetic models for methylene blue adsorption on the raw and modified clays at 25 °C

Clay	*Dye concentration (mg L^{−1})*	Q_{exp}	*Pseudo-first order parameters*			*Pseudo-second order parameters*		
			k_1	$q_{cal.}$	R^2	k_2	$q_{cal.}$	R^2
Raw clay	30	3.6	0.12	3.1	0.99	1.1	3.80	0.99
	60	7.7	0.08	6.3	0.96	1.6	11.2	0.97
	100	13.5	0.12	10.2	0.89	3.3	14.1	0.98
	200	18.1	0.09	17.4	0.93	4.1	16.9	0.95
Modified clay	30	22.1	0.33	23.2	0.74	2.5	23.3	0.99
	60	27.6	0.02	27.8	0.88	2.8	29.5	0.99
	100	55.8	0.03	56.4	0.78	3.7	53.1	0.98
	200	109.9	0.08	110.6	0.91	3.1	108.6	0.99

Table 5. Thermodynamic parameters for the adsorption of MB on the modified clay

ΔG° *(kcal mol^{−1}) at different temperatures*					ΔH° *(kcal mol^{−1})*	ΔS° *(cal mol^{−1} K^{−1})*
5 (°C)	15 (°C)	25 (°C)	35 (°C)	45 (°C)		
−7.36	−13.45	−20.15	−25.01	−34.15	−2.50	−9.38

Table 6. Comparison of adsorption capacity of MB to the various reports

Adsorbent	*Capacity (mg g^{-1})*	*Adsorption time*	*Reference*
$Zn(OH)_2$-NPs-MMT clay	259.9	3.5 min	This study
Montmorillonite clay (MMC)	289.12-293.26	30 min	Almeida et al. (2009)
Orange peel	18.6	65 min	Annadurai et al. (2002)
Clay	58.2	60 min	Gürses et al. (2006)
Spent activated clay (SAC)	78	5 h	Weng and Pan (2007)
Thermal-bentonite	14.7	16 h	Al-Asheh et al. (2003)
Kaolinite and modified clay	7.59-20.49	3 h	Ghosh and Bhattacharyya (2002)
HDTMA-MMC	166.6	60 min	Jourvand et al. (2015)
Algerian Clay	56.8	30 min	Luo et al. (2014)
AC–ZnO	32.22	120 min	Nourmoradi et al. (2015)
Fibrous clay minerals	85	100 min	Hajjaji et al. (2006)
Activated carbon	315	24 h	Yang and Qiu (2010)
CTS-g-PAA/MMT	1859	120 min	Wang et al. (2008)
Polysaccharide–clay composite bead	181.8	240 min	Uyar et al. (2016)
ST/RHA0	1885.4	60 min	de Azevedo et al. (2017)
Starch/humic acid	110	80 min	Chen et al. (2015)
Pt/Rh@GO nanocomposites	346.8	30 min	Yildiz et al. (2017)
Zinc hydroxide nanoparticles@ AC	41.49	6.5 min (Sonication time)	Ardekani et al. (2017)
Waste newspaper	611	5 min (Sonication time)	Entezari and Al-Hoseini (2007)

A modified quadratic model was used to established relationship between the removal percent and independent variables with R^2 value of 0.96. The 3D response surface and contour plots resulting from the mathematical model were used to determine the optimal conditions. Maximum adsorption was found at the optimum conditions of pH 8.0, sonication time 3.5 min, adsorbent dosage 73 mg, analyte concentration 7.5 mg L^{-1}, and electrolyte concentration 2 % w/v. Kinetic data of the adsorption process involving $Zn(OH)_2$–NPs–MMT clay conformed well to the pseudo second–order kinetic model. One of the great advantages of the prepared adsorbent is the achieving of high uptake rate. Adsorption isotherm data were treated with Langmuir, Freundlich, Temkin, and multilayer adsorption isotherm models to understand the mechanism of adsorption process. Freundlich isotherm equation can provide a good correlation to the experimental data.

The negative value of ΔH suggest an exothermic reaction. ΔG° values attained were all negative, signifying a spontaneous adsorption process. In the light of these results, it can be stated that the presented adsorbent can be well used as efficient and reliable adsorbent for treating colored solutions of MB.

Acknowledgements

This manuscript was extracted from the M.Sc. thesis of Adel Valipour (https://irandoc.ac.ir/). The financial support of this work by Islamic Azad University, Iran, Mahshahr branch, is greatly appreciated.

References

Ahenach J., Cool P., Vansant E., (1998), Acid/base treatment of Al-PILC in KCl solution, *Microporous and Mesoporous Materials*, **26**, 185-192.

Al-Asheh S., Banat F., Abu-Aitah L., (2003), The removal of methylene blue dye from aqueous solutions using activated and non-activated bentonites, *Adsorption Science & Technology*, **21**, 451-462.

Almeida C., Debacher N., Downs A., Cottet L., Mello C., (2009), Removal of methylene blue from colored effluents by adsorption on montmorillonite clay, *Journal of Colloid and Interface Science*, **332**, 46-53.

Annadurai G., Juang R.-S., Lee D.-J., (2002), Use of cellulose-based wastes for adsorption of dyes from aqueous solutions, *Journal of Hazardous Materials*, **92**, 263-274.

Antony J., Roy R.K., (1999), Improving the process quality using statistical design of experiments: a case study, *Quality Assurance: Good Practice, Regulation, and Law*, **6**, 87-95.

Araujo P.W., Brereton R.G., (1996), Experimental design III. Quantification, *TRAC Trends in Analytical Chemistry*, **15**, 156-163.

Ardekani P.S., Karimi H., Ghaedi M., Asfaram A., Purkait M.K., (2017), Ultrasonic assisted removal of methylene blue on ultrasonically synthesized zinc hydroxide nanoparticles on activated carbon prepared from wood of cherry tree: experimental design methodology and artificial neural network, *Journal of Molecular Liquids*, **229**, 114-124.

Auta M., Hameed B.H., (2014), Chitosan–clay composite as highly effective and low-cost adsorbent for batch and fixed-bed adsorption of methylene blue, *Chemical Engineering Journal*, **237**, 352-361.

Bergaya F., Lagaly G., (2006), General introduction: clays, clay minerals, and clay science, *Developments in Clay Science*, **1**, 1-18.

Bilgiç C., (2005), Investigation of the factors affecting organic cation adsorption on some silicate minerals, *Journal of Colloid and Interface Science*, **281**, 33-38.

Chen Q.-h., Fu M.-l., Liu J., Zhang H.-f., He G.-q., Ruan H., (2009), Optimization of ultrasonic-assisted extraction (UAE) of betulin from white birch bark using response surface methodology, *Ultrasonics Sonochemistry*, **16**, 599-604.

Chen D., Chen J., Luan X., Ji H., Xia Z., (2011), Characterization of anion–cationic surfactants modified montmorillonite and its application for the removal of methyl orange, *Chemical Engineering Journal*, **171**, 1150-1158.

Chen R., Zhang Y., Shen L., Wang X., Chen J., Ma A., Jiang W., (2015), Lead (II) and methylene blue removal using a fully biodegradable hydrogel based on starch immobilized humic acid, *Chemical Engineering Journal*, **268**, 348-355.

Cione A.P., Neumann M.G., Gessner F., (1998), Time-dependent spectrophotometric study of the interaction of basic dyes with clays: III. Mixed dye aggregates on SWy-1 and laponite, *Journal of Colloid and Interface Science*, **198**, 106-112.

de Azevedo A.C., Vaz M.G., Gomes R.F., Pereira A.G., Fajardo A.R., Rodrigues F.H., (2017), Starch/rice husk ash based superabsorbent composite: high methylene blue removal efficiency, *Iranian Polymer Journal*, **26**, 93-105.

Entezari M.H., Al-Hoseini Z.S.J.U.s., (2007), Sono-sorption as a new method for the removal of methylene blue from aqueous solution, **14**, 599-604.

Espantaleon A., Nieto J., Fernandez M., Marsal A., (2003), Use of activated clays in the removal of dyes and surfactants from tannery waste waters, *Applied Clay Science*, **24**, 105-110.

Ghaedi M., Khajesharifi H., Yadkuri A.H., Roosta M., Sahraei R., Daneshfar A., (2012), Cadmium hydroxide nanowire loaded on activated carbon as efficient adsorbent for removal of Bromocresol Green, *Spectrochimica Acta Part A: Molecular and Biomolecular Spectroscopy*, **86**, 62-68.

Ghaedi M., Ansari A., Sahraei R., (2013), ZnS: Cu nanoparticles loaded on activated carbon as novel adsorbent for kinetic, thermodynamic and isotherm studies of Reactive Orange 12 and Direct yellow 12 adsorption, *Spectrochimica Acta Part A: Molecular and Biomolecular Spectroscopy*, **114**, 687-694.

Ghaedi M., Khafri H.Z., Asfaram A., Goudarzi A., (2016), Response surface methodology approach for optimization of adsorption of Janus Green B from aqueous solution onto ZnO/Zn(OH)2-NP-AC: Kinetic and isotherm study, *Spectrochimica Acta Part A: Molecular and Biomolecular Spectroscopy*, **152**, 233-240.

Ghosh D., Bhattacharyya K.G., (2002), Adsorption of methylene blue on kaolinite, *Applied Clay Science*, **20**, 295-300.

Guo J.-Z., Li B., Liu L., Lv K., (2014), Removal of methylene blue from aqueous solutions by chemically modified bamboo, *Chemosphere*, **111**, 225-231.

Gürses A., Doğar Ç., Yalçın M., Açıkyıldız M., Bayrak R., Karaca S., (2006), The adsorption kinetics of the cationic dye, methylene blue, onto clay, *Journal of Hazardous materials*, **131**, 217-228.

Hajjaji M., Alami A., El Bouadili A., (2006), Removal of methylene blue from aqueous solution by fibrous clay minerals, *Journal of Hazardous Materials*, **135**, 188-192.

Hassani A., Alidokht L., Khataee A., Karaca S., (2014), Optimization of comparative removal of two structurally different basic dyes using coal as a low-cost and available adsorbent, *Journal of the Taiwan Institute of Chemical Engineers*, **45**, 1597-1607.

Hosseini S., Khosravi-Darani K., Mohammadifar M., Nikoopour H., (2009), Production of mycoprotein by Fusarium venenatum growth on modified vogel medium, *Asian Journal of Chemistry*, **21**, 4017.

Jourvand M., Shams Khorramabadi G., Omidi Khaniabadi Y., Godini H., Nourmoradi H., (2015), Removal of methylene blue from aqueous solutions using modified clay, *Journal of Basic Research in Medical Sciences*, **2**, 32-41.

Liu P., Zhang L., (2007), Adsorption of dyes from aqueous solutions or suspensions with clay nano-adsorbents, *Separation and Purification Technology*, **58**, 32-39.

Luo W.-J., Gao Q., Wu X.-L., Zhou C.-G., (2014), Removal of cationic dye (methylene blue) from aqueous solution by humic acid-modified expanded perlite: experiment and theory, *Separation Science and Technology*, **49**, 2400-2411.

Mahmoodi V., Sargolzaei J., (2014), Optimization of photocatalytic degradation of naphthalene using nano-TiO_2/UV system: statistical analysis by a response surface methodology, *Desalination and Water Treatment*, **52**, 6664-6672.

Malenović A., Dotsikas Y., Mašković M., Jančić–Stojanović B., Ivanović D., Medenica M., (2011), Desirability-based optimization and its sensitivity analysis for the perindopril and its impurities analysis in a microemulsion LC system, *Microchemical Journal*, **99**, 454-460.

Mishael Y.G., Rytwo G., Nir S., Crespin M., Annabi-Bergaya F., Van Damme H., (1999), Interactions of monovalent organic cations with pillared clays, *Journal of Colloid and Interface Science*, **209**, 123-128.

Miyamoto N., Kawai R., Kuroda K., Ogawa M., (2000), Adsorption and aggregation of a cationic cyanine dye on layered clay minerals, *Applied Clay Science*, **16**, 161-170.

Murray H.H., (2000), Traditional and new applications for kaolin, smectite, and palygorskite: a general overview, *Applied Clay Science*, **17**, 207-221.

Nassar M.M., Magdy Y.H., (1997), Removal of different basic dyes from aqueous solutions by adsorption on palm-fruit bunch particles, *Chemical Engineering Journal*, **66**, 223-226.

Nourmoradi H., Ghiasvand A., Noorimotlagh Z., (2015), Removal of methylene blue and acid orange 7 from aqueous solutions by activated carbon coated with zinc oxide (ZnO) nanoparticles: equilibrium, kinetic, and thermodynamic study, *Desalination and Water Treatment*, **55**, 252-262.

Oliveira L.C., Rios R.V., Fabris J.D., Sapag K., Garg V.K., Lago R.M., (2003), Clay–iron oxide magnetic composites for the adsorption of contaminants in water, *Applied Clay Science*, **22**, 169-177.

Porath J., Sundberg L., Fornstedt N., Olsson I., (1973), Salting-out in amphiphilic gels as a new approach to hydrophobia adsorption, *Nature*, **245**, 465-466.

Pradas E.G., Sánchez M.V., Cruz F.C., Viciana M.S., Pérez M.F., (1994), Adsorption of cadmium and zinc from aqueous solution on natural and activated bentonite, *Journal of Chemical Technology and Biotechnology*, **59**, 289-295.

Rytwo G., Nir S., Margulies L., (1995), Interactions of monovalent organic cations with montmorillonite: adsorption studies and model calculations, *Soil Science Society of America Journal*, **59**, 554-564.

Secula M.S., David E., Cagnon B., Vajda A., Stan C., Mămăligă I., (2018), Kinetics and equilibrium studies of 4-chlorophenol adsorption onto magnetic activated carbon composites, *Environmental Engineering and Management Journal*, **17**, 1783-793.

Sharma P., Borah D.J., Das P., Das M.R., (2016), Cationic and anionic dye removal from aqueous solution using montmorillonite clay: evaluation of adsorption parameters and mechanism, *Desalination Water Treatment*, **57**, 8372-8388.

Shawabkeh R.A., Tutunji M.F., (2003), Experimental study and modeling of basic dye sorption by diatomaceous clay, *Applied Clay Science*, **24**, 111-120.

Skipper N., Sposito G., Chang F.-R.C., (1995), Monte Carlo simulation of interlayer molecular structure in swelling clay minerals. 2. Monolayer hydrates, *Clays and Clay Minerals*, **43**, 294-303.

Smičiklas I.D., Milonjić S.K., Pfendt P., Raičević S., (2000), The point of zero charge and sorption of cadmium (II) and strontium (II) ions on synthetic hydroxyapatite, *Separation and Purification Technology*, **18**, 185-194.

Sun J., Li Y., Liu T., Du Q., Xia Y., Xia L., Wang Z., Wang K., Zhu H., Wu D.J.E.E., Journal M., (2014), Equilibrium, kinetic and thermodynamic studies of cationic red x-grl adsorption on graphene oxide, *Environmental Engineering and Management Journal*, **13**, 2551-2559.

Tahir S., Rauf N., (2006), Removal of a cationic dye from aqueous solutions by adsorption onto bentonite clay, *Chemosphere*, **63**, 1842-1848.

Talarposhti A.M., Donnelly T., Anderson G., (2001), Colour removal from a simulated dye wastewater using a two-phase anaerobic packed bed reactor, *Water Research*, **35**, 425-432.

Teng H., Lee W.Y., Choi Y.H., (2014), Optimization of Ultrasonic-Assisted Extraction of Polyphenols, Anthocyanins, and Antioxidants from Raspberry (Rubus coreanus Miq.) Using Response Surface Methodology, *Food Analytical Methods*, **7**, 1536-1545.

Tsai W.-T., Hsu H.-C., Su T.-Y., Lin K.-Y., Lin C.-M., Dai T.-H., (2007), The adsorption of cationic dye from aqueous solution onto acid-activated andesite, *Journal of Hazardous materials*, **147**, 1056-1062.

Tsang D.C., Hu J., Liu M.Y., Zhang W., Lai K.C., Lo I.M., (2007), Activated carbon produced from waste wood pallets: adsorption of three classes of dyes, *Water, Air, and Soil Pollution*, **184**, 141-155.

Unuabonah E., Adebowale K., Olu-Owolabi B., (2007), Kinetic and thermodynamic studies of the adsorption of lead (II) ions onto phosphate-modified kaolinite clay, *Journal of Hazardous Materials*, **144**, 386-395.

Uyar G., Kaygusuz H., Erim F.B., (2016), Methylene blue removal by alginate–clay quasi-cryogel beads, *Reactive and Functional Polymers*, **106**, 1-7.

Vasques É.d.C., Carpiné D., Dagostin J.L.A., Canteli A.M.D., Igarashi-Mafra L., Mafra M.R., Scheer A.d.P., (2014), Modelling studies by adsorption for the removal of sunset yellow azo dye present in effluent from a soft drink plant, *Environmental Technology*, **35**, 1532-1540.

Wang L., Zhang J., Wang A., (2008), Removal of methylene blue from aqueous solution using chitosan-g-poly (acrylic acid)/montmorillonite superadsorbent nanocomposite, *Colloids and Surfaces A: Physicochemical and Engineering Aspects*, **322**, 47-53.

Weng C.-H., Pan Y.-F., (2007), Adsorption of a cationic dye (methylene blue) onto spent activated clay, *Journal of Hazardous Materials*, **144**, 355-362.

Wong K.T., Eu N.C., Ibrahim S., Kim H., Yoon Y., Jang M., (2016), Recyclable magnetite-loaded palm shell-waste based activated carbon for the effective removal of methylene blue from aqueous solution, *Journal of Cleaner Production*, **115**, 337-342.

Xu H., Heinze T.M., Chen S., Cerniglia C.E., Chen H., (2007), Anaerobic metabolism of 1-amino-2-naphthol-based azo dyes (Sudan dyes) by human intestinal microflora, *Applied and Environmental Microbiology*, **73**, 7759-7762.

Xu Y.C., Tang Y.P., Liu L.F., Guo Z.H., Shao L., (2017), Nanocomposite organic solvent nanofiltration membranes by a highly-efficient mussel-inspired co-deposition strategy, *Journal of Membrane Science*, **526**, 32-42.

Xu Y.C., Wang Z.X., Cheng X.Q., Xiao Y.C., Shao L., (2016), Positively charged nanofiltration membranes via economically mussel-substance-simulated co-deposition for textile wastewater treatment, *Chemical Engineering Journal*, **303**, 555-564.

Willett C., Fu G.Y., Jackson N.M., (2019), Color removal from pulp mill effluent using coal ash produced from georgia coal combustion plants, *Environmental Engineering and Management Journal*, **18**, 945-956.

Yang J., Qiu K., (2010), Preparation of activated carbons from walnut shells via vacuum chemical activation and their application for methylene blue removal, *Chemical Engineering Journal*, **165**, 209-217.

Yazdani O., Irandoust M., Ghasemi J.B., Hooshmand S., (2012), Thermodynamic study of the dimerization equilibrium of methylene blue, methylene green and thiazole orange at various surfactant concentrations and different ionic strengths and in mixed solvents by spectral titration and chemometric analysis, *Dyes and Pigments*, **92**, 1031-1041.

Yildiz Y., Okyay T.O., Sen B., Gezer B., Kuzu S., Savk A., Demir E., Dasdelen Z., Sert H., Sen F., (2017), Highly monodisperse Pt/Rh nanoparticles confined in the graphene oxide for highly efficient and reusable sorbents for methylene blue removal from aqueous solutions, *ChemistrySelect*, **2**, 697-701.

Yu B., Zhang X., Xie J., Wu R., Liu X., Li H., Chen F., Yang H., Ming Z., Yang S.-T., (2015), Magnetic graphene sponge for the removal of methylene blue, *Applied Surface Science*, **351**, 765-771.

Zhang Y.Q., Yang X.B., Wang Z.X., Long J., Shao L., (2017), Designing multifunctional 3D magnetic foam for effective insoluble oil separation and rapid selective dye removal for use in wastewater remediation, *Journal of Materials Chemistry A*, **5**, 7316-7325.